Liquid Crystals
Publication details, including instructions for authors and subscription information:
http://www.informaworld.com/smpp/title~content=t713926090

Optical behaviour of cholesteric liquid crystal cells with novel photoisomerizable chiral dopants

Jui-Hsiang Liu[a]; Po-Chih Yang[b]; Yu-Kan Wang[b]; Chien-Chih Wang[b]
[a] Department of Chemical Engineering, and Institute of Electro-optics, National Cheng Kung University, Tainan, Taiwan 70101, Roc [b] Department of Chemical Engineering, National Cheng Kung University, Tainan, Taiwan 70101, Roc

To cite this Article Liu, Jui-Hsiang , Yang, Po-Chih , Wang, Yu-Kan and Wang, Chien-Chih(2006) 'Optical behaviour of cholesteric liquid crystal cells with novel photoisomerizable chiral dopants', Liquid Crystals, 33: 3, 237 — 248
To link to this Article: DOI: 10.1080/02678290600577971
URL: http://dx.doi.org/10.1080/02678290600577971

Liquid Crystals, Vol. 33, No. 3, March 2006, 237–248

Taylor & Francis
Taylor & Francis Group

Optical behaviour of cholesteric liquid crystal cells with novel photoisomerizable chiral dopants

JUI-HSIANG LIU*†, PO-CHIH YANG‡, YU-KAN WANG‡ and CHIEN-CHIH WANG‡

†Department of Chemical Engineering, and Institute of Electro-optics, National Cheng Kung University, Tainan, Taiwan 70101, Roc

‡Department of Chemical Engineering, National Cheng Kung University, Tainan, Taiwan 70101, Roc

(*Received 3 November 2005; accepted 1 December 2005*)

In order to investigate the effect of photoisomerization of *E–Z* structures on the optical behaviour of cholesteric liquid crystal (ChLC) cells, a series of novel azo derivatives was synthesized. Molecular structures were identified using ^{1}H NMR, ^{13}C NMR, FTIR and elemental analysis. Thermal properties and the specific rotation of the synthesized chiral azo derivatives were estimated. Rubbed polyvinyl alcohol coated on the inner surface of substrates was used to control the liquid crystal alignment in cells. The effect of chiral dopants on the reflection band of ChLC cells was investigated, as well as the dependence of polarizing optical microscope textures on temperature. The stability and reproducibility of the effect of UV irradiation on the cell reflection band and real image recording were confirmed. Real image recording of the ChLC cells fabricated in this investigation was also studied; a photoinduced image through a mask is given. Photoirradiated and non-irradiated areas appear as different reflected colours leading to the formation of an image. Stacking of the ChLC cells was found to intensify the brightness of the reflection band.

1. Introduction

Due to the presence of molecular chirality, cholesterically ordered material has regions which selectively reflect circularly polarized electromagnetic radiation over a band of wavelengths. The central wavelength (λ_0) band reflected wavelength is determined by the pitch (p) of the molecular helix, according to $\lambda_0=\bar{n}\times p$, where $\bar{n}$ is the average refractive index of the cholesterically ordered material. The bandwidth $\Delta\lambda$ is given by $\Delta\lambda=p\times\Delta n$, where Δn is the birefringence of the uniaxially oriented phase corresponding to the cholesterically ordered phase. In the visible range, the regions selectively reflect circularly polarized light of a particular colour [1–4]. Typically, with Δn being less than about 0.15 and n of the order 1, the bandwidth in the visible range of the spectrum is 60 to 90 nm [5–8].

Because the cholesteric layer absorbs no radiation incident upon it, it is not only a colour- and circularly polarized light-selective reflector, but also a filter which selectively transmits light of opposite handedness within the reflection band. Outside its reflection band, the cholesterically ordered material is transparent and transmits both polarization components [9–12].

By partially converting the convertible compound in the irradiated regions of the layer, the pitch of the molecular helix in the layer, and thus the colour, is altered in these regions. The difference in pitch between the first and second regions is proportional to the difference in the amount of convertible compound in the converted state and/or the non-converted state between the first and the second region [13–16].

Azobenzene derivatives used as photochromic liquid crystals have been explored as photonic materials, because they can change not only their own optical properties but also the optical anisotropy of the surrounding liquid crystal molecules by photoirradiation [17]. *Trans-cis* photoisomerization of the azobenzene molecules in the liquid crystal phase can disorganize the phase structure of liquid crystal molecules, resulting in a liquid crystal to isotropic isothermal phase transition [18, 19]. The photochemical phase transition of liquid crystals has been examined conveniently by transmission and reflection mode analyses [20–24].

In a previous study, we reported on the electro-optical control of light passing through a polymer/liquid crystal composite film [25, 26]. In these systems, the phase separation of polymer in a liquid crystal led to the formation of domains of focal-conic texture. In the

*Corresponding author. Email: jhliu@mail.ncku.edu.tw

Liquid Crystals
ISSN 0267-8292 print/ISSN 1366-5855 online © 2006 Taylor & Francis
http://www.tandf.co.uk/journals
DOI: 10.1080/02678290600577971

absence of an electric field, the focal-conic structure was formed and caused light scattering. When an electric field was applied to the polymer stabilized cholesteric texture (PSCT) cells, the liquid crystal director reoriented parallel to the direction of the applied field, and the PSCT cells became transparent.

In principle, the specific rotation reveals the characteristics of the net vector of the polarity of the chiral molecules on the planarly polarized light. The 'polar effect' should also affect host liquid crystal molecules. The results of both polar and steric interactions between chiral dopants and host liquid crystals are revealed as the helical twisting power (HTP) [27–34]. In this study, we synthesized some novel azo derivatives and studied their effect on cholesteric liquid crystals (ChLCs). The thermal stability and optical properties of the fabricated ChLC cells were investigated. Brightness enhancement due to the stacking of the cells was also confirmed.

2. Experimental

2.1. *Measurements*

FTIR spectra were recorded on a Jasco VALOR III (Tokyo, Japan) FTIR spectrophotometer. Nuclear magnetic resonance (NMR) spectra were obtained on a Bruker AMX-400 (Darmstadt, Germany) high resolution NMR spectrometer. Optical rotations were measured at 30°C in $CHCl_3$ using a Jasco DIP-370 polarimeter with the sodium D-line ($\lambda = 589$ nm). The measurements were performed using 1% solutions in $CHCl_3$. Differential scanning calorimetry (DSC) was conducted with a Perkin-Elmer DSC 7 at heating and cooling rates of 10 K min^{-1} under nitrogen. The phase transitions were investigated by polarizing optical microscope (POM), using an Olympus BH-2 microscope equipped with a Mettler hot stage FP-82, and the temperature scanning rate was determined at a rate 5–10 K min^{-1}.

UV spectroscopy measurements were carried out with a Jasco V-550 UV-VIS spectrophotometer. X-ray diffraction (XRD) data were recorded on a Rigaku Rint 2500 series instrument with Ni-filtered CuK_α radiation. The sample in a quartz capillary was held in a temperature-controlled cell (Rigaku LC high temperature controller). The transmittance spectra were recorded with a USB-2000 fibre optic spectrometer from Oceanoptics Co. UV light (365 nm) with an intensity of 0.4 mW was used as a pumping light to induce isomerization of azo molecules in the ChLC systems.

2.2. *Materials*

ZLI-2293, a commercially available eutectic mixture of several low molecular mass nematic liquid crystals, was

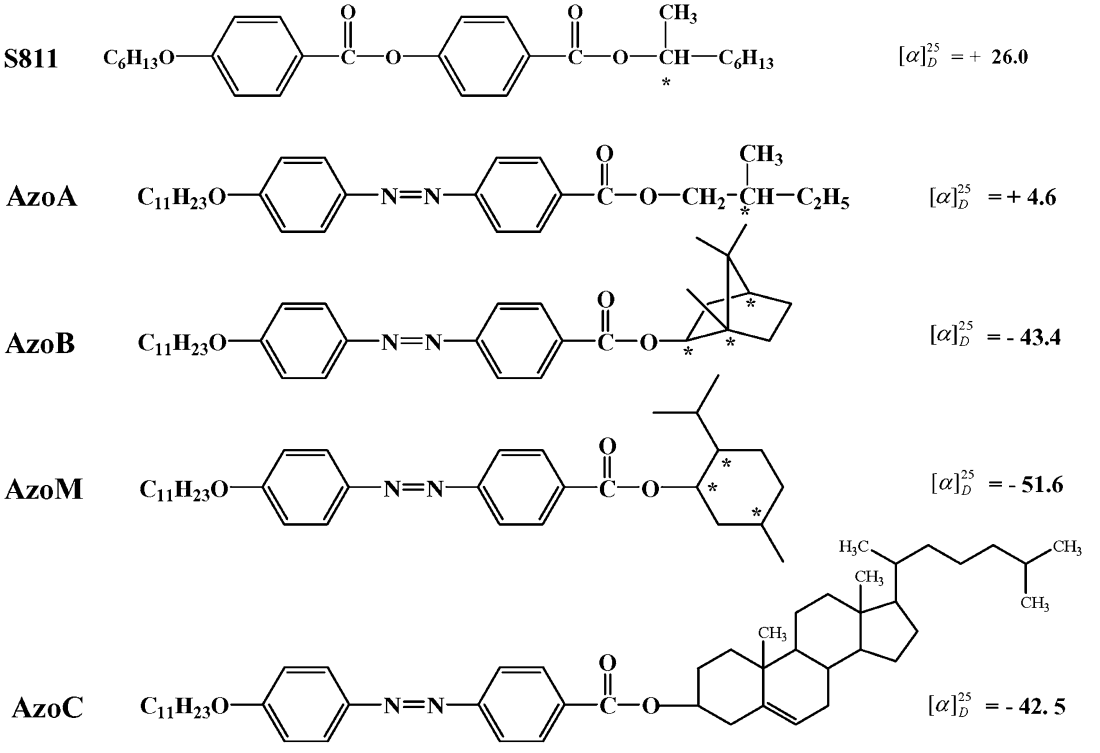

Scheme 1.

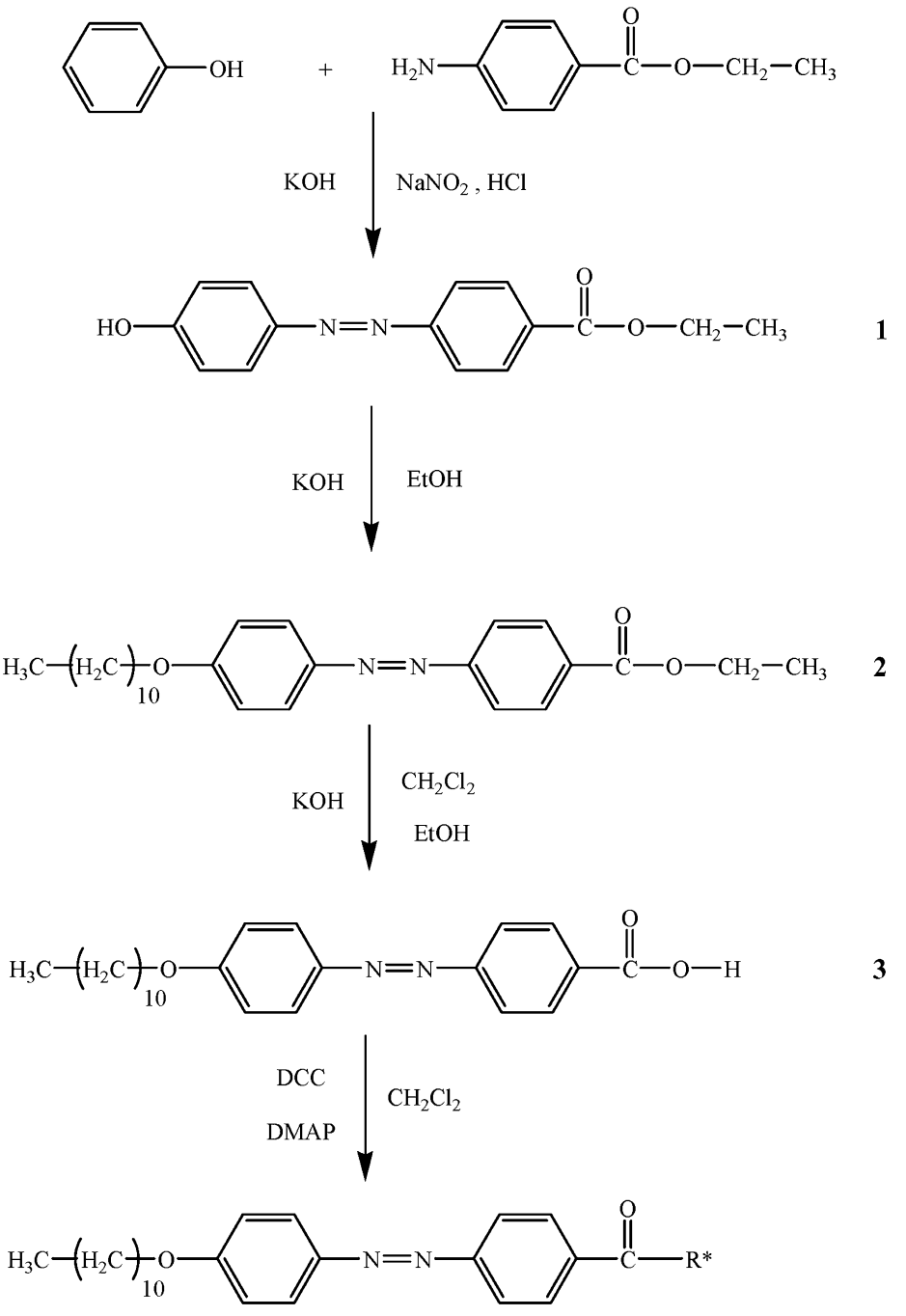

R* = (+)- 2-Methyl butyloxyl **AzoA**
(-)- Bornyl **AzoB**
(-)- Menthyl **AzoM**
(-)- Cholesternyl **AzoC**

Scheme 2.

purchased from Merck (Darmstadt, Germany) and was used as a host LC without further purification. This LC shows a nematic phase over a wide range of temperature to 85°C. Chiral and azobenzene compounds used in this investigation are shown in scheme 1 and were synthesized as indicated in scheme 2. The products were identified spectrophotometercally. Chiral agent S811 (Merck, Germany), which induces a left-handed helical optical rotation, was dissolved in the host nematic liquid crystal (NLC) to produce a ChLC phase. We synthesized AzoA, AzoB, AzoM, and AzoC azobenzene derivatives containing chiral (−)-amyl, (−)-bornyl, (−)-menthyl and (−)-cholesteryl groups, respectively. The LC properties of the mixtures were examined by POM, DSC and XRD. The LC mixtures were injected into a glass cell having a 15 μm cell gap; the cells consisted of pairs of glass plates coated with PVA (polyvinyl alcohol, M_w=20 000) and rubbed to provide homogeneous molecular orientation.

2.3. *Ethyl 4-(4-hydroxy-phenylazo)benzoate (1)*

Ethyl 4-aminobenzoate (10 g, 60.6 mmol) was dissolved in 1M aqueous HCl (100 ml) and kept in an ice bath at 0°C. $NaNO_2$ (4.2 g, 60.8 mmol), dissolved in water (30 ml), was added dropwise to the solution and the mixture stirred for 30 min. Sodium hydroxide (7.2 g, 0.18 mol) and phenol (5.8 g, 61.7 mmol) were dissolved in water (80 ml) and the solution stirred for 30 min at 0°C; the former solution was then added dropwise to the latter solution. The mixture was held at 0°C and stirred for 1 h. The resulting mixture was poured into water and the solution neutralized with 5% aqueous HCl. The precipitated crude product was filtered and recrystallized twice from ethanol. Yield: 11.8 g (72%), T_m=153–154°C. FTIR (cm^{-1}): 3399 (OH), 2973, 2927, 2906 (CH_2), 1693 (C=O in Ar–COO–), 1601, 1504 (C–C in Ar). ^1H NMR ($CDCl_3$, δ in ppm): 1.38 (t, 3H, OCH_2CH_3), 4.35 (d, 2H, OCH_2), 7.03–8.17 (m, 8H, aromatic).

2.4. *Ethyl 4-(4-undecyloxyphenylazo)benzoate (2)*

Compound **1** (8.1 g, 30 mmol) was dissolved in DMF (70 ml), and potassium hydroxide (2.52 g, 45 mmol), dissolved in DMF (50 ml), added dropwise to this solution. Potassium iodide (0.83 g, 5 mmol) and 1-bromoundecane (7.76 g, 33 mmol), dissolved in DMF (20 ml), was then added. The mixture was heated to 80°C and held at that temperature for 24 h with stirring, it was then poured into water and the mixture extracted twice with $CHCl_3$. After evaporation, the crude product was recrystallized twice from ethanol. Yield: 9.42 g (74%), T_m=100–101°C. FTIR (cm^{-1}): 2950, 2855 (CH_2), 1690 (C=O in Ar–COO–).^1H NMR (acetone-d6, δ in ppm): 0.88–0.85 (m, 3H, CH_3), 1.07–1.22 (m, 18H, –CH_2), 1.37–1.40 (t, 3H, OCH_2CH_3), 4.02 (d, 2H, OCH_2Ph), 4.15 (d, 2H, OCH_2), 7.05–7.08 (d, 2H, aromatic), 7.78–7.92 (m, 4H, aromatic), 8.12–8.16 (d, 2H, aromatic).

2.5. *4-(4-Undecyloxyphenylazo)benzoic acid (3)*

Compound **2** (10.6 g, 25.0 mmol) was dissolved in ethanol (60 ml), and potassium hydroxide (10 g, 178.5 mmol), dissolved in ethanol, was then added and the mixture heated at reflux for 6 h. The resulting suspension was poured into water, and the solution neutralized with dilute HCl. It was extracted twice with $CHCl_3$, and the extract washed with water, dried over magnesium sulphate, and evaporated. Yield: 8.03 g (81%). FTIR (cm^{-1}): 2945, 2852 (CH_2), 1689 (C=O in Ar–COO–). ^1H NMR (acetone-d6, δ in ppm): 0.87–1.97 (m, 21H, –$C_{10}H_{21}$), 4.04 (d, 2H, OCH_2Ph), 7.10–7.12 (d, 2H, aromatic), 7.86–7.94 (m, 4H, aromatic), 8.12–8.14 (d, 2H, aromatic).

2.6. *(+)-Amyl 4-(4-undecyloxyphenylazo)benzoate (AzoA)*

Compound **3** (3.96 g, 10 mmol) and amyl alcohol (0.97 g, 11 mmol) were dissolved in CH_2Cl_2 (30 ml) at room temperature; DCC (3.09 g, 15.0 mmol) and DMAP (0.12 g, 1 mmol) were then added to the solution, and the mixture was stirred for 24 h at 30°C. It was then washed with water, dried over $MgSO_4$, and evaporated. The crude product was purified by column chromatography (silica gel, ethyl acetate/hexane=1/5) and recrystallized from ethanol. Yield: 2.47 g (53%), T_m=85.5°C. FTIR (cm^{-1}): 2954, 2860 (CH_2), 1702 (C=O in Ar–COO–). ^1H NMR ($CDCl_3$, δ in ppm): 0.83–0.96 (m, 9H, CH_3), 0.96–1.48 (m, 21H, CH_2), 4.03 (d, 2H, CH_2OPh), 4.08 (d, 2H, COO CH_2), 7.00–7.02 (d, 2H, aromatic), 7.89–7.98 (m, 4H, aromatic), 8.15–8.17 (d, 2H, aromatic). ^{13}C NMR (100.6 MHz, $CDCl_3$): 11.29, 14.10, 16.55, 22.67, 25.99, 29.32, 34.31, 68.43, 69.76, 114.78, 122.31, 125.17, 130.50, 131.50, 146.84, 155.35, 162.31, 166.22. Anal: calcd for $C_{29}H_{42}N_2O_3$, C 74.68, H 9.01, N 6.01; found C 74.57, H 9.13, N 6.05%.

Compounds AzoB, AzoC, and AzoM were synthesized in a similar manner.

2.7. *(−)-Bornyl 4-(4-undecyloxyphenylazo)benzoate (AzoB)*

Yield: 2.23 g (42%), T_m=105.4°C. FTIR (cm^{-1}): 2950, 2865 (CH_2), 1710 (C=O in Ar–COO–). ^1H NMR (400 MHz, $CDCl_3$, δ in ppm): 0.86–0.98 (m, 12H, CH_3), 1.12–2.50 (m, 27H, CH_2), 4.03–4.07 (d, 2H,

CH_2O), 5.12–5.16 (s, 1H, Ar–COOCH), 7.00–7.03 (d, 2H, aromatic), 7.89–7.96 (m, 4H, aromatic), 8.16–8.19 (d, 2H, aromatic). ^{13}C NMR (100.6 MHz, $CDCl_3$): 13.63, 14.10, 18.92, 19.73, 27.42, 28.09, 29.32, 31.89, 36.91, 44.99, 47.90, 49.13, 68.43, 80.81, 114.78, 122.31, 125.18, 130.46, 131.53, 146.85, 155.33, 162.30, 166.37. Anal: calcd for $C_{34}H_{48}N_2O_3$, C 76.69, H 9.02, N 5.26; found C 76.78, H 9.11, N 5.21%.

2.8. *(−)-Cholesteryl 4-(4-undecyloxyphenylazo) benzoate (AzoC)*

Yield: 3.13 g (41%), T_m=123.4°C. FTIR (cm^{-1}): 2936, 2852 (CH_2), 1699 (C=O in Ar–COO–). ^1H NMR (400 MHz, $CDCl_3$, δ in ppm): 0.70–1.08 (m, 18H, CH_3), 1.27–2.50 (m, 46H, CH_2), 4.03–4.07 (d, 2H, CH_2O), 4.87 (s, 1H, Ar–COOCH), 5.43 (s, 1H, C=CH), 6.98–7.02 (d, 2H, aromatic), 7.88–7.95 (m, 4H, aromatic), 8.15–8.18 (d, 2H, aromatic). ^{13}C NMR (100.6 MHz, $CDCl_3$): 22.68, 23.84, 24.29, 25.99, 27.89, 28.23, 29.33, 31.90, 36.18, 38.22, 39.51, 39.73, 42.32, 50.04, 56.14, 56.69, 68.42, 74.85, 114.77, 122.25, 122.83, 125.16, 130.51, 131.82, 139.60, 146.85, 155.27, 162.29, 165.52, 168.30. Anal: calcd for $C_{51}H_{76}N_2O_3$, C 80.10, H 9.95, N 3.66; found C 79.97, H 9.98, N 3.75%.

2.9. *(−)-Menthyl 4-(4-undecyloxyphenylazo)benzoate (AzoM)*

Yield: 1.17 g (22%). T_m=71.7°C. FTIR (cm^{-1}): 2955, 2862 (CH_2), 1706 (C=O in Ar–COO–). ^1H NMR (400 MHz, $CDCl_3$, δ in ppm): 0.75–0.82 (m, 12H, CH_3), 0.93–2.17 (m, 9H, CH_2), 4.04–4.06 (d, 2H, CH_2O), 4.93–4.98 (s, 1H, Ar–COOCH), 7.00–7.02 (d, 2H, aromatic), 7.89–7.95 (m, 4H, aromatic), 8.15–8.17 (d, 2H, aromatic). ^{13}C NMR (100.6 MHz, $CDCl_3$): 14.11, 16.55, 20.77, 22.68, 23.66, 25.99, 26.53, 29.33, 29.56, 31.90, 34.31, 40.97, 47.27, 68.43, 75.11, 114.78, 122.28, 125.18, 130.52, 131.84, 146.83, 155.28, 162.30, 165.65. Anal: calcd for $C_{34}H_{50}N_2O_3$, C 76.40, H 9.36, N 5.24; found C 76.28, H 9.41, N 5.29%.

2.10. *Fabrication of liquid crystal cells*

ITO plates were cleaned with detergent solution, then washed with water and acetone using ultrasonic equipment for 20 min and 60 min, respectively. After completion of the cleaning process, the plates were dried in vacuum. One side surface was coated with polyvinyl alcohol (M_w=20 000), dried and then rubbed. A glass cell with a pair of parallel pre-rubbed ITO plates and 12 μm gap was fabricated. After filling with LC mixture, the cell was sealed with epoxy resin. The optical properties of the LC cells were then investigated.

3. Results and discussion

In order to study the optical properties and steric structures of chiral compounds having different chiral moieties which affect the light reflection band of ChLC cells, a series of chiral azobenzene derivatives were synthesized (see schemes 1 and 2). From the molecular structure, 4, 4-substituted compounds show a relatively linear structure. Without the structural disturbance from the benzene ring, the steric effects due to variations between the rod like *Z*-form and the bent *E*-form of azo derivatives can be estimated. The synthesized products were identified using ^1H NMR, FTIR, and elemental analyses. Figure 1 shows the ^{13}C NMR spectrum of AzoM in $CDCl_3$. The chirality of AzoM was estimated using an automatic digital polarimeter.

The phase transition temperatures and the specific rotation of the azobenzene derivatives were estimated using DSC and polarimetry, respectively. The results are summarized in table 1. The specific rotation of AzoA is right-handed; the others, AzoB, AzoC, and AzoM are all have left-handed optical activity. The azobenzene derivatives in table 1 do not show liquid crystal phases. The variation between heating and cooling cycles may be due to the delay of molecular reorientation. As can be seen in scheme 1, the difference in steric hindrance between the chiral compounds is quite large.

Figure 2 shows the effects of UV irradiation on the UV-vis spectra of sample cells with various azobenzene derivatives. All azobenzene derivatives in the *E*-form showed a strongly absorbing band in the UV region (~360 nm) which is attributed to the π–π^* transition, and a weakly absorbing band in the visible region (~450 nm) due to the n–π^* transition. The *E*-form is generally more stable than the *Z*-form, but each isomer can be converted into the other by light-irradiation of the appropriate wavelength. UV irradiation caused a decrease at around 360 nm and an increase at around 450 nm. For derivative AzoM, as shown in figure 2 (*c*), the *E*–*Z* transition was completely achieved in 35 s. As shown in scheme 1, the specific rotation of the AzoM was the largest. The results suggest that both optical rotation ability and steric hindrance of the asymmetric moieties of the chiral dopants are the factors that chiefly affect their UV sensitivity.

The dependence of the specific rotation of the azobenzene derivatives on the UV irradiation is shown in figure 3. In principle, UV irradiation causes *E*-*Z* isomerization of the azo bond which leads to a variation in polarity at the chiral centre. The specific rotation of AzoA was 4.6°; UV irradiation seems not to affect it, suggesting that *E*-*Z* variation in AzoA causes no

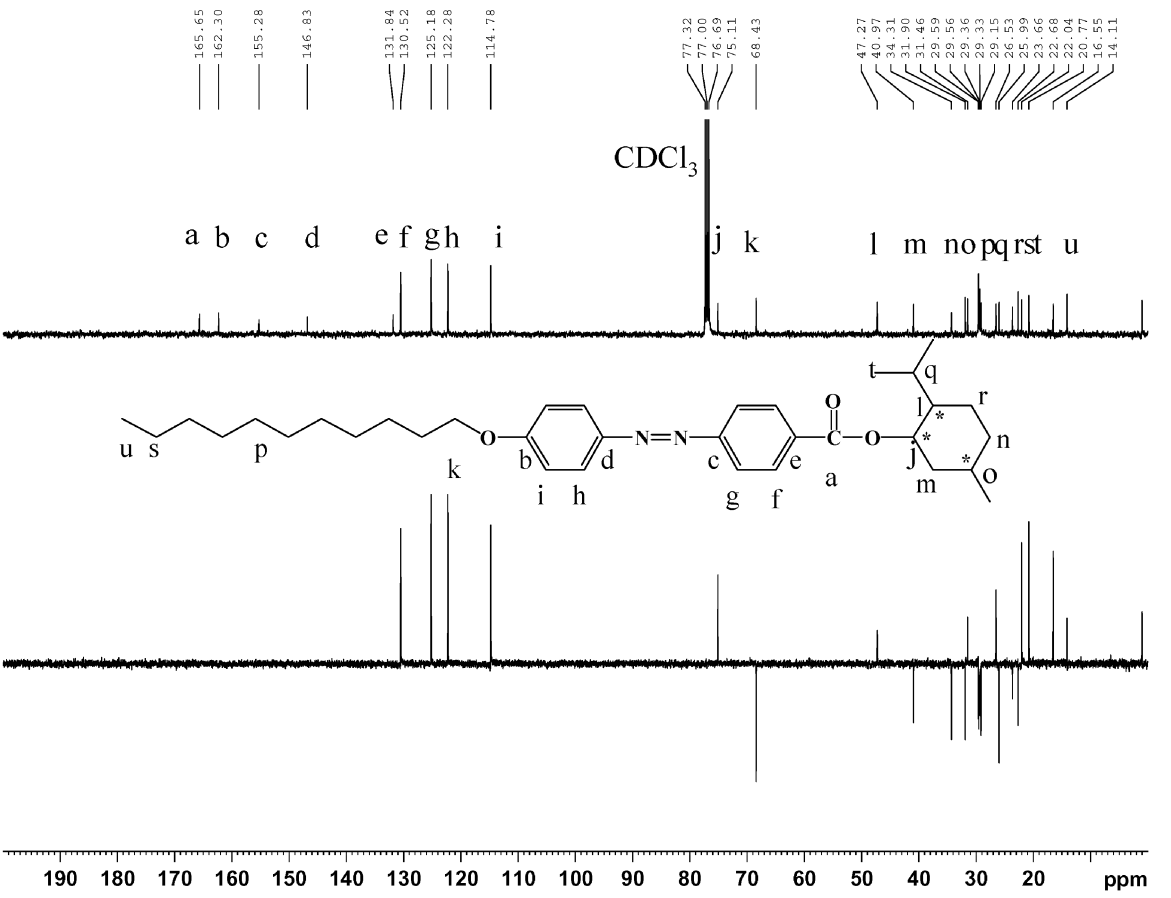

Figure 1. ^{13}C NMR spectrum of AzoM in $CDCl_3$.

significant change in polarity at the chiral centre. However, AzoB and AzoM exhibited significant variations after the UV irradiation. For AzoC, as compared with AzoB and AzoM, a relatively small variation was seen. This may be due to the presence of the bulky cholesteryl group which contains many chiral centres. Since some of the chiral centres in AzoC are more remote from the isomeric change than are the chiral centres in AzoB and AzoM, the impact of isomerization on the polarity transfer is smaller. As can be seen in the molecular structures shown in scheme 1, variation of the terminal chiral groups affected the polarity of the molecules and caused much variation in specific rotation between the compounds.

The effects of the chiral dopants on the reflection wavelength, the pitch, and phase transition temperature of the sample cells are summarized in table 2. The ChLC cells were prepared using commercially available ZLI-2293/S811 with various amounts and kinds of azobenzene derivatives as dopants. The main wavelength (λ_0) and pitch of the cells before and after UV irradiation were estimated. As can be seen in table 2, for sample cells 4 and 5, AzoA and AzoB could organize the arrangement of the NLC as a helix structure with no

Table 1. Phase transition temperature (°C), enthalpy changes ($J\,g^{-1}$) and specific rotation of chiral compounds: Cr=crystal, I=isotropic.

Sample	Heating	Cooling	$[\alpha]_D^{25}$ [a]
AzoA	Cr 85.5 (105.3) I	I 71.6 (−104.1) Cr	+4.6
AzoB	Cr 105.4 (55.9) I	I 87.1 (−56.2) Cr	−43.4
AzoC	Cr 123.4 (29.4) I	I 48.3 (−11.9) Cr	−42.5
AzoM	Cr 71.7 (64.8) I	I 42.8 (−62.4) Cr	−51.6

[a] Specific rotation of compounds, 0.1 g in 10 ml $CHCl_3$.

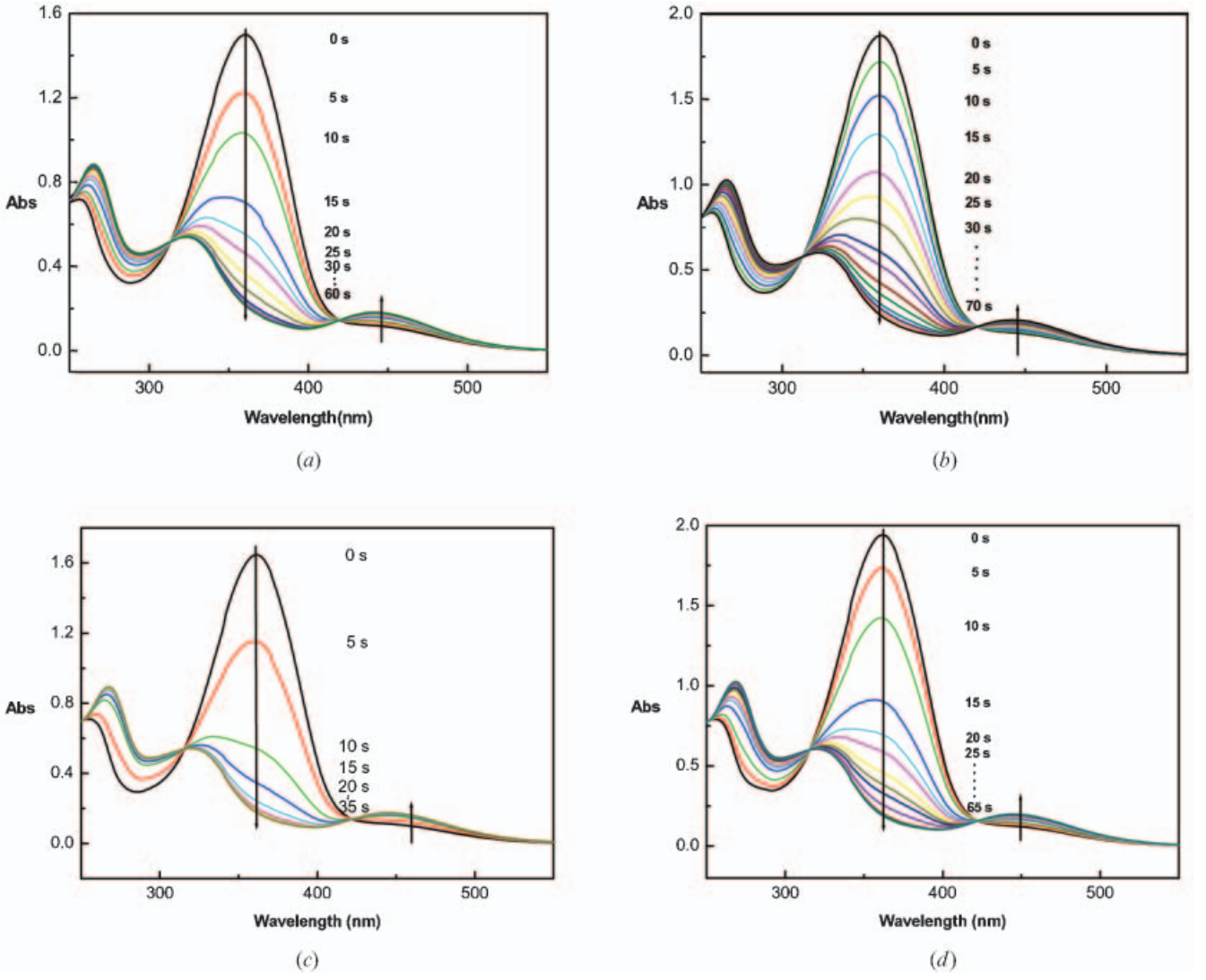

Figure 2. UV spectra of compounds (*a*) AzoA, (*b*) AzoB, (*c*) AzoM, and (*d*) AzoC in chloroform, before and after UV irradiation.

added chiral S811. Comparing cell 2 with cells 6 to 9, AzoA and AzoB lengthened the pitch of the cells; however, AzoC and AzoM shortened the pitch of the cells. These results suggest that the chiral dopants significantly affected the pitch of the cells, independently of the specific rotation of the chiral dopants. This case may be similar to the relationship between *R*/*S*-configuration and (+)/(−)-specific rotation, in which they are all independent.

Right/left 'specific rotation' reveals the polar effect of chiral dopants on planar polarized light, which may be rotated in a right/left-handed direction due to asymmetry of the chiral molecules. The polarity should also affect liquid crystals. Helical twisting power reveals the net intermolecular polar effects existing in ChLCs. Depending on the molecular interactions, in some cases, polar factors from both 'specific rotation' and 'helical twisting power' may work in the same direction and show higher effects on the 'twisting' of liquid crystal molecules. However, in other cases, the two factors may work in opposite directions and cancel each other out. Nevertheless, from the theory of enantiomers, it is clear that enantiomeric chiral dopants should show opposite effects on the same host LC molecules. For a pair of enantiomers, the *R*-form and *S*-form enantiomeric isomers usually exhibit opposite effects. As described in the literature [5] opposing effects of S811 and R811 on cholesteric pitch were observed, S811 and R811 are mirror image enantiomers.

It is clear that without examination we can predict nothing about the effect of chiral dopants on the helical twisting and induced helical direction of the sample

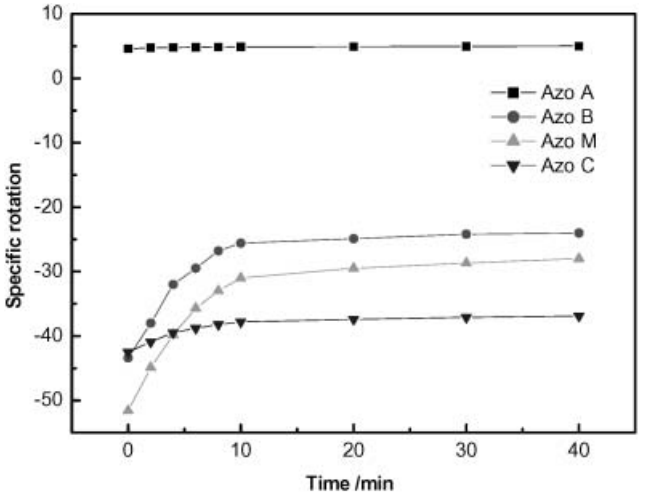

Figure 3. Effect of UV irradiation on specific rotations of Azo compounds.

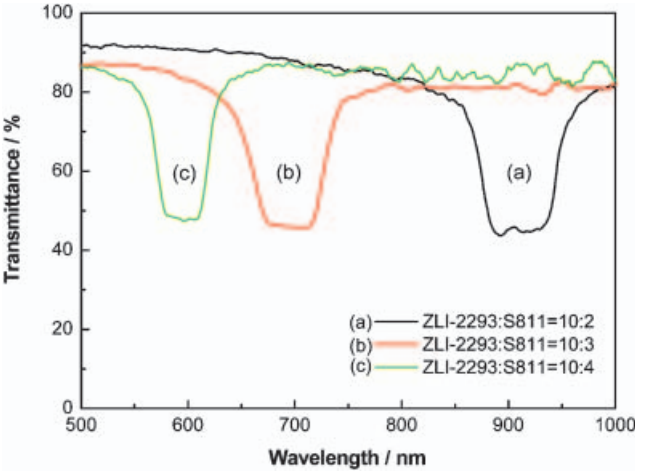

Figure 4. Effects of doping amount of S811 on reflection band (cells 1–3).

cells. As can be seen in table 2, for cells 10 to 13, an increase of the added amount of S811 and azo derivatives further decreased the pitch of the cells to certain levels. Measurements of $T_{Ch\text{-}I}$ indicate that an addition of chiral dopants lowered the clearing points of the ChLC cells. The presence of chiral dopants may disturb the orientational order of the LCs, leading to a decrease of clearing temperature. Furthermore, the azo derivatives in this investigation are all photoisomerizable compounds. Irradiation with UV light might induce the formation of a bent structure of the azobenzene derivatives leading to a variation in the reflection wavelength. For cells 1 to 3, dopant S811 is not a photoisomerizable compound, so UV irradiation could not cause any variation in the reflected band.

Figure 4 shows the effect of chiral dopant on the reflective band of the ChLC cells. An increase in the S811 concentration caused a blue shift, the reflection band being shifted from the IR to the visible region. These results suggest that the addition of the chiral dopant shortened the pitch of the cholesteric liquid crystal cells.

In order to investigate the thermal dependence of reflection in the cells, ChLC cells were treated at various temperatures, The results summarized in figure 5. The reflected light was shifted to a shorter wavelength region and the bandwidth of the reflected light peak was narrowed with increasing temperature. The results suggest that the orientation of the LC molecules was affected by the rise in temperature. A further increase in temperature led to the formation of an isotropic phase.

Table 2. Effects of chiral dopants and UV irradiation on reflection band of cholesteric cells.

Cell	Chiral dopant	Weight ratio ZLI-2293/S811	λ_0/nm[a]		Pitch/nm		HTP/μm^{-1}		$T_{Ch\text{-}I}$/°C[b]	
			before	after	before	after	before	after	heating	cooling
1	–	10/2	920	920	588	588	10.2	10.2	77	76
2	–	10/3	695	695	444	444	9.8	9.8	72	72
3	–	10/4	596	596	381	381	10.0	10.0	66	65
4	AzoA	10/4[c]	1035	1056	661	675	5.3	5.2	87	86
5	AzoB	10/4[c]	1050	1080	671	691	5.2	5.1	88	88
6	AzoA	10/3/0.5	712	686	455	438	8.5	8.8	67	66
7	AzoB	10/3/0.5	820	785	524	502	7.4	7.7	69	69
8	AzoC	10/3/0.5	658	646	420	413	9.2	9.3	71	70
9	AzoM	10/3/0.5	628	714	401	456	9.6	8.5	63	63
10	AzoA	10/4/0.5	588	546	376	349	8.6	9.2	60	59
11	AzoB	10/4/0.5	654	581	418	371	7.7	8.7	61	60
12	AzoC	10/4/0.5	536	523	342	334	9.4	9.6	64	63
13	AzoM	10/4/0.5	502	543	321	347	10.0	9.3	58	57

[a] Reflection band before and after UV irradiation. [b] $T_{Ch\text{-}I}$: clearing temperature, estimated using DSC at 10 K min^{-1} in a nitrogen atmosphere. [c] With no S811.

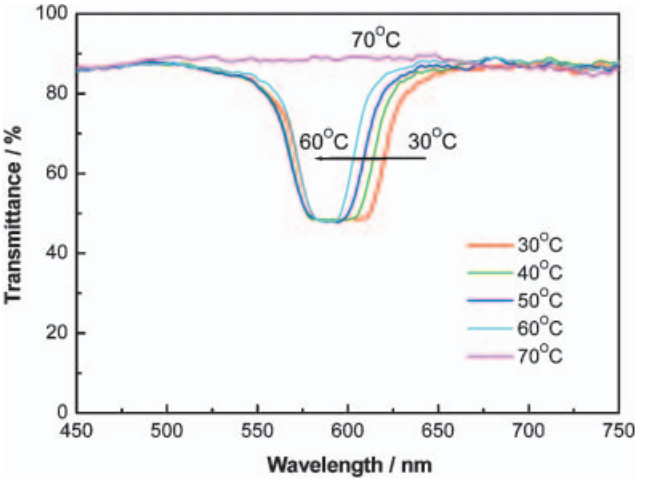

Figure 5. Dependence of UV-vis spectra on temperature (ZLI-2293/S811 = 10/4).

The coloured reflected light vanished completely when the cell was heated above the clearing point ($T_{Ch\text{-}I}$) of 66°C, and the cell became transparent.

The pitch change and molecular orientation of the LCs could be confirmed using POM. In order to study the dependence of the POM texture on the variation of cholesteric pitch, a cell with no alignment layers was fabricated. Figure 6 shows the change in colours and pattern of POM textures of the ChLC cell at different temperatures. In theory, the variation of pitch changes the reflection bandwidth, brightness, and colours of the cells.

Figure 7 shows POM textures of the ChLC cell at different temperatures. In this case, the surfaces of the substrates were treated with orientation film and rubbed in a parallel direction. Accordingly, many planar domain boundaries were found in the textures. The dependence of the POM textures on temperature is seen in the with different coloured patterns. An increase of temperature increased the density of the boundaries. On the change to isotropic liquid, the dark picture shown in figure 7 (*c*) was obtained. On comparing the POM textures in figures 6 and 7, the effect of the rubbed alignment layer on the surfaces of the substrates can be seen. The arrangement of the LCs in each cell is different. As shown in figure 7, the presence of boundaries indicates the formation of planar domains; in Figure 6, only a continual characteristically coloured texture with no boundary could be seen.

Commercially available ZLI-2293 with chiral S811 was used as the host LC. The effects of the chiral compounds synthesized in this investigation on the host ChLC cells were investigated, with results shown in figure 8. Lengthening of the LC pitches caused a red shift, while shortening of the pitches caused a blue shift.

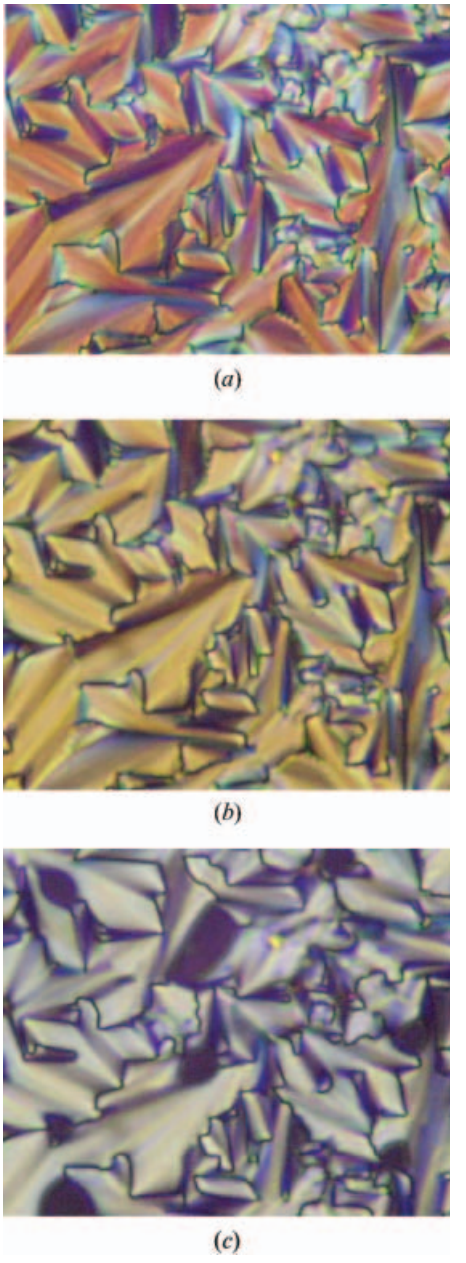

Figure 6. POM textures at (*a*) 30°C, (*b*) 45°C, (*c*) 60°C (ZLI-2293/S811 = 10/4) (× 100).

Increasing the S811 concentration strengthened the HTP of the cells which led to the blue shifts. The phase change and molecular orientation of the LCs could be confirmed by POM.

As can be seen in figure 9 (*a*), UV irradiation caused a blue shift. After 3 min, of UV irradiation no further shift could be obtained. The results suggest that the *Z*-form of AzoB might shorten the pitch of the ChLC. The bendt structure of the *Z*-form molecule might reduce

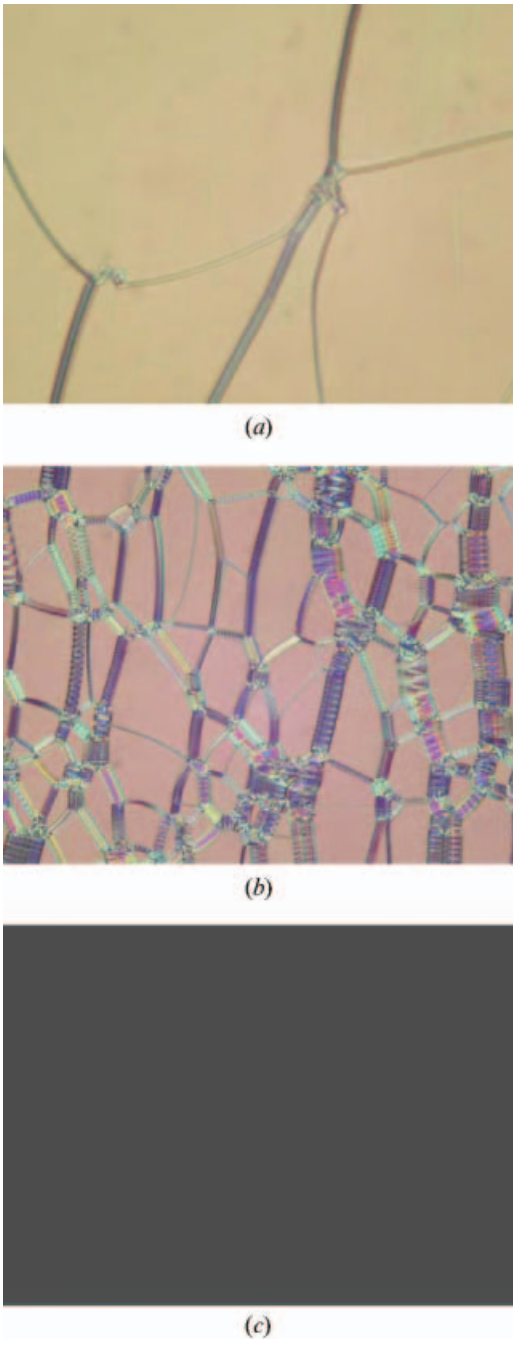

Figure 7. Planar textures of a ChLC cell at (*a*) 30°C, (*b*) 60°C, (*c*) 80°C (ZLI-2293/S811/AzoC=10/3/0.5) (× 100).

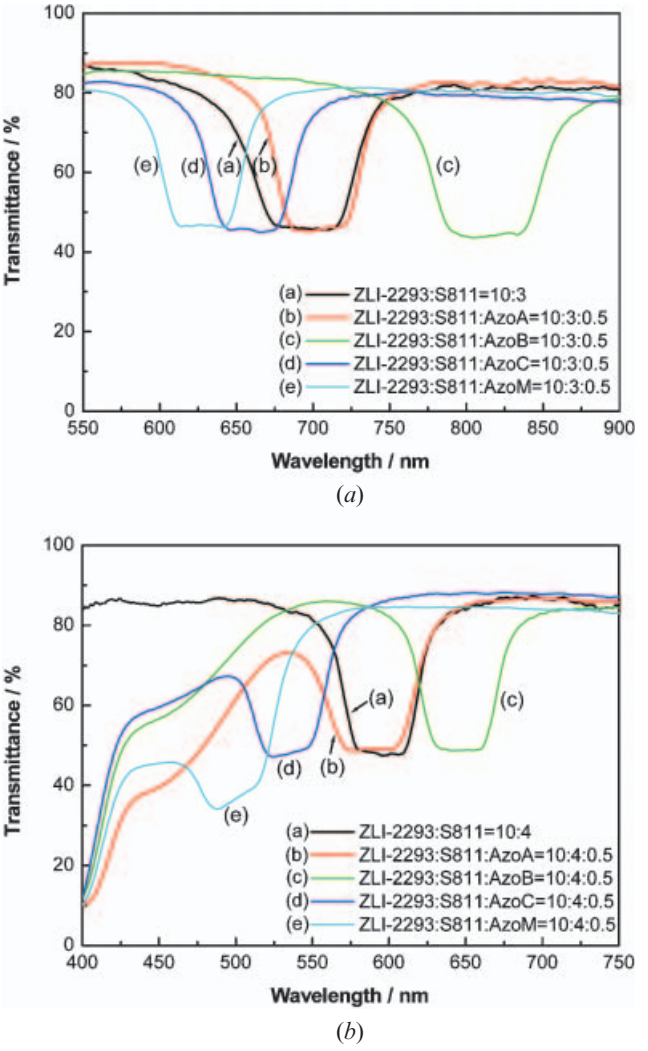

Figure 8. Effect of chiral dopants on the reflection band of LC cells with (*a*) 10/3, and (*b*) 10/4 ZLI-2293/S811 as host component.

the free volume of the LC. However, *E*/*Z* conformational change may also alternate molecular polarity and HTP leading to the decrease in helical pitch. From the spectra, variation at 633 nm before and after UV irradiation can be expected from digital data recording. Figure 9 (*b*) shows a repeaed on/off variation at 633 nm and the reproducibility of the cycles. The results suggest that UV irradiation isomerized AzoB from the *E*-form to the *Z*-form structure and shortened the pitch of the liquid crystal. Thermal treatment returned the AzoB to the original *E* form structure and lengthened the pitch to its original size. Figure 10 shows the dynamic recording of UV irradiation of the ChLC cell. After UV irradiation, the transmittance of the cell at 633 nm increased. The cell was then treated at 50°C to ensure the return of the AzoB from *Z*- to *E*-form. When we compare the rate of the blue shift in the ZLI-2293/S811/AzoB cell in figure 9 (*a*) with the rate of isomerization of AzoB by itself in figure 1 (*b*), the blue shift speed is not very different. This suggests that the HTP of the cell in figure 9 (*a*) is directly correlated with the isomerization of the azo compound.

Real image recording of the ChLC cell with the composition of ZLI-2293/S811/AzoB=10/4/0.5 was

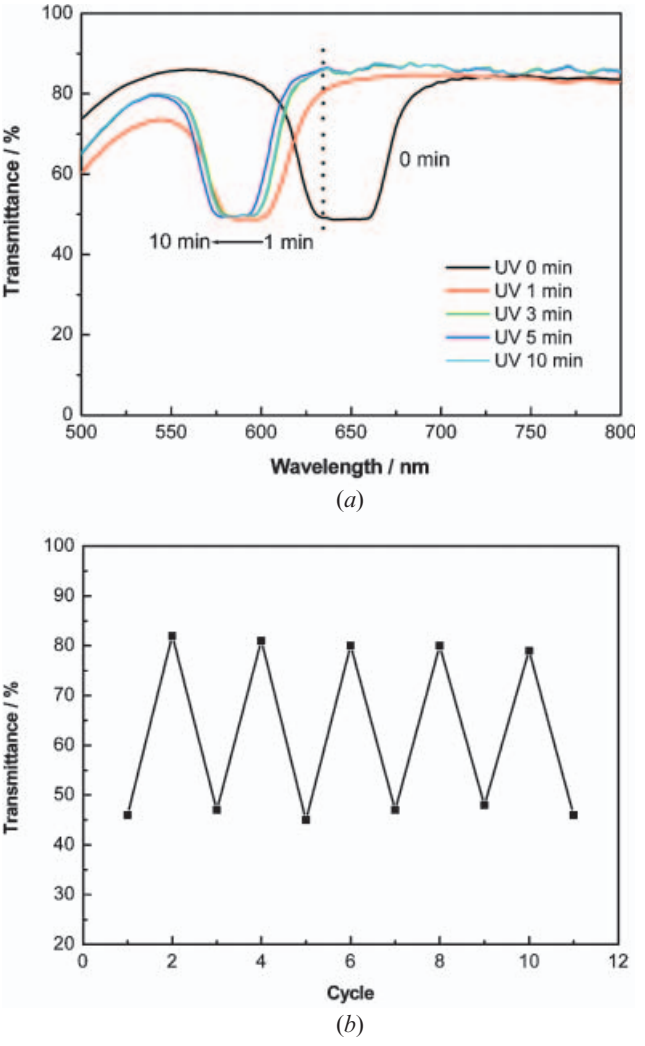

Figure 9. (*a*) Effect of UV irradiation on cholesteric cells; (*b*) reproducibility of UV irradiation for ZLI-2293/S811/AzoB=10/4/0.5 cell.

performed. Figure 11 (*a*) shows the appearance of the reflected colour of the cells before and after UV irradiation; figure 11 (*b*) shows the result for a cell irradiated through a mask. The lighter colour at the periphery of the letters might be due to diffraction of the UV light through the mask. Figure 12 shows the spectral addition of stacked ChLC cells. After stacking, the reflection band is just the additional bandwidth of each cell. The results suggest that stacking of three R, G, B reflected cells can broaden the bandwidth to full visible light, which leads to a white light reflection. In principle, the white light reflection film could be used in LC displays to enhance the back lighting efficiency of a display.

Up to now, the real mechanism of molecular interaction between chiral dopants and LCs has not been clear. It was found that the bendt *Z*-form molecule

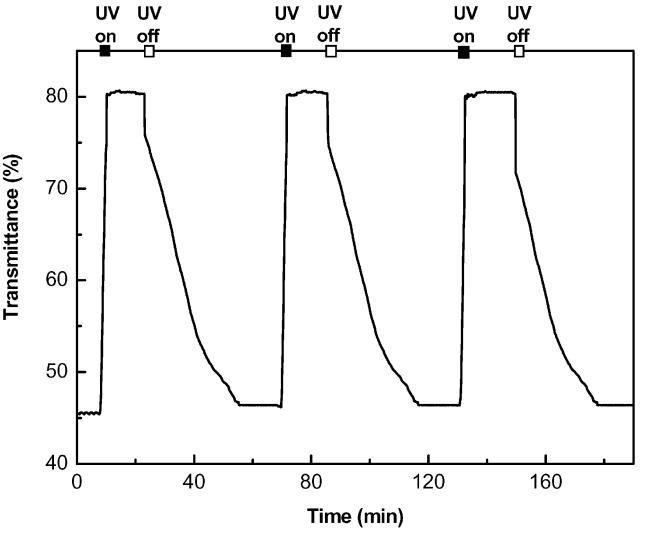

Figure 10. Dynamic recording of UV irradiation of a ChLC cell detected at 633 nm.

could cause both blue shift [15, 16, 22, 35] and red shift [18, 22, 23, 36]. From the molecular structure, the bendt *Z*-azo structure may disturb the order of the arrangement of LCs. However, the polarity and steric environment of the whole molecule should also be considered. For every case, the results of the blue/red shift reveal the final balance of the steric and polarity factors in the systems. A study of the polarity and steric factors on the induction of cholesteric helical structure from a nematic arrangement is now in progress.

4. Conclusions

A series of chiral azo derivatives were synthesized. The effects of the chiral dopants on ChLC cells were studied. The specific rotation of the chiral compounds was found to be affected by UV irradiation. The reflection band of the ChLC cells was shifted by UV irradiation due to the *E-Z* conformational change of the azo dopants. The stability and reproducibility of the photo-induced variation in UV-vis spectrum were confirmed. Real image recording of the cholesteric cells was achieved using UV irradiation through a mask. Stacking of the ChLC cells was found to intensify the brightness of the reflection band.

Acknowledgements

The authors would like to thank the National Science Council (NSC) of the Republic of China (Taiwan) for financial support for this research under Contract No. NSC 93-2216-E006-001.

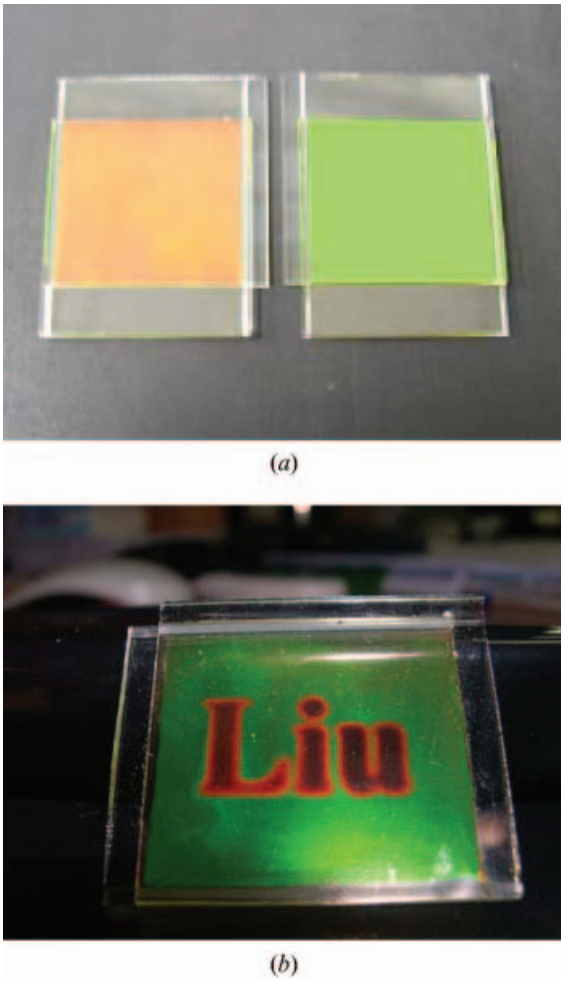

Figure 11. (*a*) Liquid crystal cells before and after UV irradiation; (*b*) real image recording through a mask. (ZLI-2293/S811/AzoB=10/4/0.5).

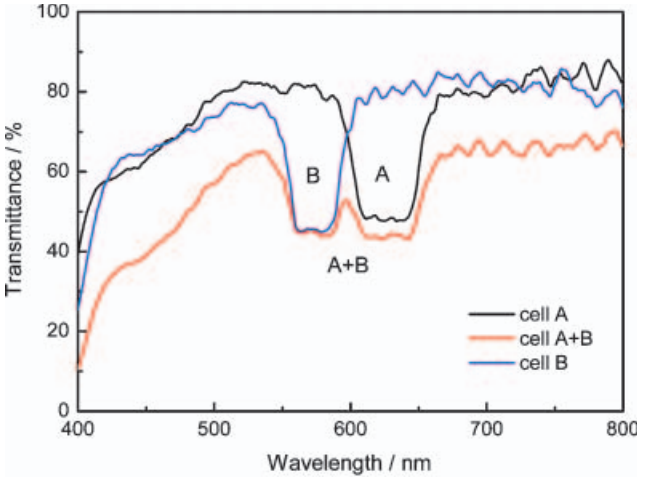

Figure 12. UV-vis spectra of stacked cells: A with ZLI-2293/S811/AzoB=10/4/0.5 before UV irradiation, and B with the same composition after UV irradiation. Cell (A+B) denotes stacking of the cells.

References

[1] H.K. Lee, K. Doi, H. Harada, O. Tsutsumi, A. Kanazawa, T. Shiono, T. Ikeda. *J. phys. Chem. B.*, **104**, 7023 (2000).
[2] N. Tamaoki, A.V. Parfenov, A. Masaki, H. Matsuda. *Adv. Mater.*, **9**, 1102 (1997).
[3] M. Brehmer, J. Lub, P. van de Witte. *Adv. Mater.*, **10**, 1438 (1998).
[4] D. Demus, J. Goodby, G. Grey, H. Spiess, V. Vill (Eds), *Handbook of Liquid Crystals*, Wiley, New York (1998).
[5] D.J. Broer, J. Lub, G.N. Mol. *Nature*, **378**, 467 (1995).
[6] A. Boudet, C. Binet, M. Mitov, C. Bourgrette, E. Boucher. *Eur. Phys. J. E.*, **2**, 247 (2000).
[7] R.A.M. Hikmet, H. Kemperman. *Nature*, **392**, 476 (1998).
[8] A. Lavernhe, M. Mitov, C. Binet, C. Bourgerette. *Liq. Cryst.*, **28**, 803 (2001).
[9] P.G. de Gennes, J. Prost. *The Physics of Liquid Crystals*, pp. 263–280, Clarendon Press, Oxford (1993).
[10] S. Elston, R. Sambles (Eds), *The Optics of Thermotropic Liquid Crystals*, Taylor & Francis, London (1998).
[11] R.A. Delden. *Controlling Molecular Chirality and Motion* Chap. 3, Baarn, Holland; Electronic Version: ISBN 90-367-1609-3 (2002).
[12] N. Tamaoki. *Adv. Mater.*, **13**, 1135 (2001).
[13] P. van de Witte, M. Brehmer, J. Lub. *J. mater. Chem*, **9**, 2087 (1999).
[14] A.Y. Bobrovsky, N.I. Boiko, V.P. Shibaev, J. Springer. *Adv. Mater.*, **12**, 1180 (2000).
[15] C. Ruslim, K. Ichimura. *J. phys. Chem. B.*, **104**, 6529 (2000).
[16] H.K. Lee, K. Doi, H. Harada, O. Tsutsumi, A. Kanazawa, T. Shiono, T. Ikeda. *J. phys. Chem.*, **104**, 7023 (2000).
[17] E. Sackman. *J. Am. chem. Soc.*, **93**, 7088 (1971).
[18] C. Ruslim, K. Ichimura. *Adv. Mater.*, **13**, 37 (2001).
[19] C. Ruslim, K. Ichimura. *Adv. Mater.*, **13**, 641 (2001).
[20] J.H. Liu, P.C. Yang. *J. appl. polym. Sci.*, **91**, 3693 (2004).
[21] J.H. Liu, H.Y. Wang. *J. appl. polym. Sci.*, **91**, 789 (2004).
[22] S. Kurihara, S. Nomiyama, T. Nonaka. *Chem. Mater.*, **12**, 9 (2000).
[23] S. Kurihara, S. Nomiyama, T. Nonaka. *Chem. Mater.*, **13**, 1992 (2001).
[24] T. Yoshioka, T. Ogata, A.M. Zahangir, T. Nonaka, S. Kurihara. *Liq. Cryst.*, **31**, 15 (2004).
[25] J.H. Liu, H.Y. Wang. *J. appl. polym. Sci.*, **91**, 789 (2004).
[26] J.H. Liu, F.T. Wu. *J. polym. Res.*, **11**, 43 (2004).
[27] J.H. Liu, C.D. Hsieh. *J. appl. polym. Sci.* (to be published) (2005).
[28] J.H. Liu, P.C. Yang. *Liq. Cryst* (to be published) (2005).
[29] J.H. Liu, P.C. Yang, Y.G. Fuh. *Appl. Phys. Lett.*, **86**, 161120 (2005).
[30] J.H. Liu, H.J. Hung. *Liq. Cryst.*, **32**, 133 (2005).
[31] H. Baessler, M.M. Labes. *J. Chem. Phys.*, **52**, 631 (1970).
[32] G. Solladie, R. Zimmermann. *Angew. Chem., int. Ed. Engl.*, **23**, 348 (1984).
[33] R.P. Lemieux. *Acc. chem. Res.*, **34**, 845 (2001).
[34] G. Gottarelli, G.P. Spada. In *Materials-Chirality*, M.M. Green, R.J.M. Nolte, E.W. Meijer (Eds), p. 425, Volume 24 of Topics in Stereochemistry, Wiley, Hoboken, NJ (2003).
[35] S. Pieraccini, S. Masiero, G.P. Spada, G. Gottarelli. *Chem. Commun.*, 598–599 (2003).
[36] S.V. Serak, E.O. Arikainen, H.F. Gleeson, V.A. Grozhik, J.P. Guillou, N.A. Usova. *Liq. Cryst.*, **29**, 19 (2002).